Bioorganic Chemistry 90 (2019) 103030

Contents lists available at ScienceDirect

Bioorganic Chemistry

journal homepage: www.elsevier.com/locate/bioorg

Isolation and characterization of three pairs of indolediketopiperazine enantiomers containing infrequent *N*-methoxy substitution from the marine algal-derived endophytic fungus *Acrostalagmus luteoalbus* TK-43

Jin Cao[a,b], Xiao-Ming Li[a], Ling-Hong Meng[a], Belma Konuklugil[c], Xin Li[a,d], Hong-Lei Li[a,d], Bin-Gui Wang[a,d,*]

[a] Key Laboratory of Experimental Marine Biology, Institute of Oceanology, Chinese Academy of Sciences, and Laboratory of Marine Biology and Biotechnology, Qingdao National Laboratory for Marine Science and Technology, Nanhai Road 7, Qingdao 266071, People's Republic of China
[b] University of Chinese Academy of Sciences, Yuquan Road 19A, Beijing 100049, People's Republic of China
[c] Department of Pharmacognosy, Faculty of Pharmacy, Ankara University, 06110 Ankara, Turkey
[d] Center for Ocean Mega-Science, Chinese Academy of Sciences, Nanhai Road 7, Qingdao 266071, People's Republic of China

ARTICLE INFO

Keywords:
Acrostalagmus luteoalbus
N-methoxy
Indolediketopiperazine enantiomers
Anti-acetylcholinesterase activity
Anti-microbial activity

ABSTRACT

Three pairs of new *N*-methoxy-containing indolediketopiperazine enantiomers, acrozines A–C (**1**–**3**), were isolated from the culture extract of *Acrostalagmus luteoalbus* TK-43, an endophytic fungus obtained from the marine green alga *Codium fragile*. The optical resolution of compounds **1**–**3** by chiral HPLC successfully afforded individual enantiomers (+)-**1**/(–)-**1**, (+)-**2**/(–)-**2**, and (+)-**3**/(–)-**3**, respectively. The structures of all these compounds were established on the basis of detailed interpretation of their NMR and mass spectroscopic data. X-ray crystallographic analysis confirmed the structures of compounds **1**–**3**, while the absolute configurations were determined by TDDFT-ECD calculations. All these compounds containing a *N*-methoxy group which is uncommon in indolediketopiperazines. The enantiomers, (+)-**2**/(–)-**2**, showed different antimicrobial activities against several plant-pathogenic fungi, while (+)-**1** displayed better inhibitory activity against acetylcholinesterase than that of (–)-**1**.

1. Introduction

Algae are one class of the major sources of marine derived fungi, and marine algicolous fungi have attracted considerable attention for natural product research [1]. A number of new natural products have been characterized from marine algicolous fungi, with diversified chemical structures including polyketides, terpenoids, polyketide-terpenoids, peptides, and alkaloids [2–8]. In continuation of our research on structurally unique and biologically active compounds from marine algal-derived endophytic fungi [9–11], we performed chemical investigations on the culture extract of *Acrostalagmus luteoalbus* TK-43, an endophytic fungus isolated form the fresh tissue of the marine green alga *Codium fragile*. In previous studies, two new indolediketopiperazines luteoalbusins A and B, along with eight known ones, were isolated from the deep sea isolate of *A. luteoalbus* SCSIO F457 by Zhang and co-workers in 2012 [12]. In 2018, three epipolythiodioxopiperazines were reported from another marine-derived isolate of the fungus [13], which proved that *A. luteoalbus* is a prolific source of diketopiperazines. In our present work, three pairs of new indolediketopiperazine (IDT) enantiomers, namely, (±)-acrozines A–C ((±)-**1** ~ (±)-**3**), were isolated from the culture extract of the fungus (Fig. 1). All these compounds contain a *N*-methoxy group in the molecules. Indolediketopiperazines are commonly discovered from various fungal strains but *N*-methoxy-containing IDTs were only reported in one paper by Zhu and co-workers in 2012 [14]. The structures of all isolated compounds in the current work were established by extensive analysis of spectroscopic data and X-ray crystallographic analysis, whereas their absolute configurations were determined by quantum chemical ECD calculations. Compounds **1**–**3** were evaluated for antibacterial activities against human and aquatic pathogenic bacteria and plant-pathogenic fungi. The inhibitory activity against acetylcholinesterase (AChE) was also tested. This paper describes the

* Corresponding author at: Key Laboratory of Experimental Marine Biology, Institute of Oceanology, Chinese Academy of Sciences, and Laboratory of Marine Biology and Biotechnology, Qingdao National Laboratory for Marine Science and Technology, Nanhai Road 7, Qingdao 266071, People's Republic of China (B.-G. Wang).
E-mail address: wangbg@ms.qdio.ac.cn (B.-G. Wang).

https://doi.org/10.1016/j.bioorg.2019.103030
Received 15 February 2019; Received in revised form 26 April 2019; Accepted 2 June 2019
Available online 05 June 2019

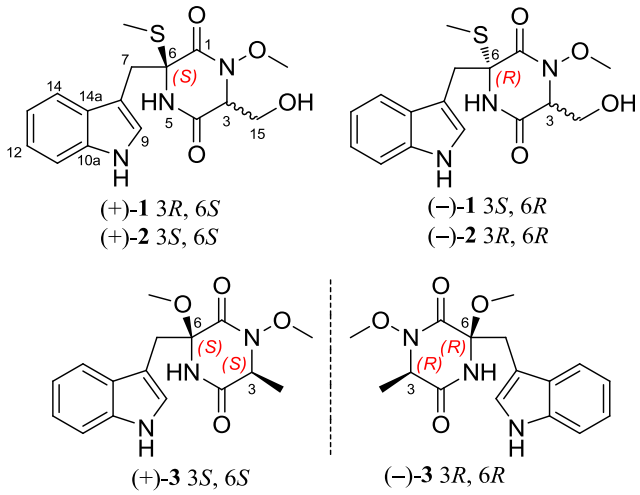

Fig. 1. The structures of compounds (±)-**1** ~ (±)-**3**.

isolation, structure determination, chiral HPLC separation, stereochemical assignment, and biological activity of the isolated compounds.

2. Experimental

2.1. General experimental procedures

Melting points were determined with an SGW X-4 micromelting-point apparatus. Optical rotations were measured on an Optical Activity AA-55 polarimeter. UV spectra were measured on a PuXi TU-1810 UV–visible spectrophotometer. ECD spectra were acquired on a Chirascan spectropolarimeter. 1D and 2D NMR spectra were recorded at 500 and 125 MHz for ^{1}H and ^{13}C, respectively, on a Bruker Avance 500 spectrometer with tetramethylsilane as internal standard. Mass spectra were obtained on a VG Autospec 3000 or an API QSTAR Pulsar 1 mass spectrometer. Analytical and semi-preparative HPLC were performed using a Dionex HPLC system equipped with a P680 pump, an ASI-100 automated sample injector, and a UVD340U multiple wavelength detector controlled by Chromeleon software (version 6.80). Commercially available Si gel (200–300 mesh, Qingdao Haiyang Chemical Co.), Lobar LiChroprep RP-18 (40–63 μm, Merck), and Sephadex LH-20 (Pharmacia) were used for open column chromatography. All solvents were distilled prior to use.

2.2. Fungal material

Acrostalagmus luteoalbus TK-43 was isolated from the fresh tissue of the marine green alga *Codium fragile* collected in Sinop, Turkey, in May 2015, using a protocol described in our precious report [15]. The alga sample was identified according to morphological characteristics by Bulent Gozcelioglu, a marine biologist form the Scientific and Technological Research Council of Turkey. The fungus was identified using a molecular biological protocol by DNA amplification and sequencing of the ITS region, as described in our previous report [15]. The sequence data derived from the fungal strain have been deposited at GenBank (accession no. MH836621). A BLAST search result showed that the sequence was most similar (99%) to the sequence of *A. luteoalbus* (accession no. KC311495.1). The strain is preserved at the Key Laboratory of Experimental Marine Biology, Institute of Oceanology, Chinese Academy of Sciences (IOCAS).

2.3. Fermentation

The modified PDB liquid medium and rice solid medium were used for small-scale fermentation to compare and select the appropriate culture medium. The HPLC profiles (Fig. S37, Supplementary material) showed that metabolites in rice medium were more abundant than that in PDB medium. Therefore, rice solid medium was selected and submitted to large-scale fermentation for chemical investigation.

For chemical investigation, the fresh mycelia of *A. luteoalbus* TK-43 were initially grown on PDA medium at 28 °C for 4 days and then were used as seed culture to be inoculated for 40 days at room temperature in 1 L conical flasks with solid rice medium (each flask contained 70 g rice, 0.2 g corn flour, 0.3 g peptone, 0.5 g yeast extract, 0.1 g sodium glutamate, 0.1 g methionine, 70 mg magnesium sulfate heptahydrate, 2 mg ferrous sulfate heptahydrate, and 100 mL naturally sourced and filtered seawater, which was obtained from the Huiquan Gulf of the Yellow Sea near the campus of IOCAS, pH 6.5–7.0).

2.4. Isolation

The whole fermented cultures (100 flasks) were extracted three times with EtOAc, and the solvents were evaporated under reduced pressure to afford an extract (45 g), which was fractionated by vacuum liquid chromatography (VLC) on silica gel eluting with different solvents of increasing polarity from petroleum ether (PE) to MeOH to yield nine fractions (Frs. 1–9) that were pooled based on TLC and HPLC analysis. Fr. 6 (13.3 g), eluted with CH_2Cl_2–MeOH (20:1), was further purified by column chromatography (CC) over Lobar LiChroprep RP-18 with a MeOH–H_2O gradient (from 10:90 to 100:0) to afford seven subfractions (Fr. 6.1–6.7). Fr. 6.1 (1.5 g) was further purified by CC on silica gel eluting with a CH_2Cl_2-MeOH gradient (from 100:1 to 10:1) and then by CC on Sephadex LH-20 (MeOH) obtained compounds (±)-**1** (76.7 mg) and (±)-**2** (60.3 mg). The optical resolution of (±)-**1** by chiral HPLC (CHIRALPAK IC, *n*-hexane–isopropanol: 70:30, 1.5 mL/min) afforded optical isomers (+)-**1** (2.5 mg) and (–)-**1** (2.7 mg), whereas the optical resolution of (±)-**2** by chiral HPLC (CHIRALPAK IC, *n*-hexane–isopropanol: 90:10, 1.0 mL/min) afforded optical isomers (+)-**2** (2.0 mg) and (–)-**2** (2.3 mg). Further purification of Fr. 6.3 (596 mg) by preparative TLC (plate: 20 × 20 cm, developing solvents: PE–acetone, 2:1) and then by CC on Sephadex LH-20 (MeOH) yielded (±)-**3** (7.4 mg), which was separated by chiral HPLC (CHIRALPAK IC, *n*-hexane–isopropanol: 80:20, 1.5 mL/min) obtained (+)-**3** (1.0 mg) and (–)-**3** (1.3 mg).

2.4.1. Compound (±)-1

Colorless single crystal (CH_2Cl_2–MeOH, 1:1); mp 235–237 °C; $[\alpha]_D^{20}$ 0 (*c* 0.08, MeOH); UV (MeOH) λ_{max} (log ε) 219 (4.31), 281 (3.44), 289 (3.37) nm; ^{1}H and ^{13}C NMR data, Table 1; ESIMS *m/z* 350.12 $[M+H]^+$, 372.10 $[M+Na]^+$; HRESIMS *m/z* 350.1161 $[M+H]^+$ (calcd for $C_{16}H_{20}N_3O_4S$, 350.1169), 372.0990 $[M+Na]^+$ (calcd for $C_{16}H_{19}N_3O_4SNa$, 372.0988).

(+)-Acrozine A [(+)-**1**]: $[\alpha]_D^{20}$ + 33 (*c* 0.06, MeOH); ECD (0.37 mM, MeOH) λ_{max} ($\Delta\varepsilon$) 214 (+2.52), 237 (+6.19), 297 (–0.63) nm.

(–)-Acrozine A [(–)-**1**]: $[\alpha]_D^{20}$ –33 (*c* 0.06, MeOH); ECD (0.60 mM, MeOH) λ_{max} ($\Delta\varepsilon$) 215 (–0.85), 237 (–5.80), 292 (+0.44) nm.

2.4.2. Compounds (±)-2

Colorless single crystal (CH_2Cl_2–MeOH, 1:1); mp 237–239 °C; $[\alpha]_D^{20}$ 0 (*c* 0.10, MeOH); UV (MeOH) λ_{max} (log ε) 219 (4.32), 281 (3.47), 289 (3.40) nm; ^{1}H and ^{13}C NMR data, Table 1; ESIMS *m/z* 350.11 $[M+H]^+$, 372.10 $[M+Na]^+$; HRESIMS *m/z* 372.0990 $[M+Na]^+$ (calcd for $C_{16}H_{19}N_3O_4SNa$, 372.0988).

(+)-Acrozine B [(+)-**2**]: $[\alpha]_D^{20}$ + 50 (*c* 0.04, MeOH); ECD (1.32 mM, MeOH) λ_{max} ($\Delta\varepsilon$) 206 (+3.73), 213 (+3.11), 239 (+5.74), 286 (–0.39) nm.

(–)-Acrozine B [(–)-**2**]: $[\alpha]_D^{20}$ –50 (*c* 0.04, MeOH); ECD (0.95 mM, MeOH) λ_{max} ($\Delta\varepsilon$) 207 (–3.69), 213 (–3.09), 240 (–5.80), 287 (+0.38) nm.

2.4.3. Compound (±)-3

Colorless single crystal (CH_2Cl_2–MeOH, 1:1); mp 215–217 °C; $[\alpha]_D^{20}$ 0

Table 1
NMR data for compounds (±)-1 ~ (±)-3 in DMSO-d_6 (^{1}H at 500 MHz, ^{13}C at 125 MHz).

	(±)-1		(±)-2		(±)-3	
Position	δ_C, type	δ_H (J in Hz)	δ_C, type	δ_H (J in Hz)	δ_C, type	δ_H (J in Hz)
1	162.6, C		162.0, C		160.3, C	
3	63.5, CH	4.37, br s	62.7, CH	3.50, br s	55.9, CH	3.60, m (overlap)
4	165.0, C		164.0, C		166.8, C	
6	66.7, C		67.7, C		87.5, C	
7	33.6, CH_2	3.21, d (14.7) 3.60, d (14.7)	35.9, CH_2	3.10, d (13.9) 3.55, d (13.9)	34.5, CH_2	3.03, d (14.0) 3.46, d (13.8)
8	107.1, C		107.3, C		106.3, C	
9	125.0, CH	7.20, s	125.3, CH	7.07, s	125.2, CH	7.04, s
10a	135.6, C		135.6, C		135.7, C	
11	111.0, CH	7.30, d (8.0)	111.0, CH	7.29, d (8.0)	111.1, CH	7.29, d (8.0)
12	120.7, CH	7.03, t (7.5)	120.8, CH	7.02, t (7.4)	120.8, CH	7.02, t (7.6)
13	118.2, CH	6.95, t (7.4)	118.4, CH	6.95, t (7.4)	118.3, CH	6.94, t (7.5)
14	118.8, CH	7.60, d (7.9)	119.2, CH	7.64, d (7.9)	119.0, CH	7.61, d (7.9)
14a	127.8, C		127.2, C		127.3, C	
15	58.5, CH_2	3.58, br s	57.6, CH_2	3.59, d (11.0) 3.65, dd (5.2, 10.3)	17.3, CH_3	1.29, d (6.8)
2-OMe	61.0, CH_3	3.67, s	60.3, CH_3	3.19, s	60.5, CH_3	3.16, s
6-SMe	12.5, CH_3	2.15, s	12.5, CH_3	2.18, s		
6-OMe					50.6, CH_3	3.16, s
5-NH		8.60, s		8.94, s		8.95, s
10-NH		10.91, s		10.94, s		10.94, s
15-OH		4.94, t (5.1)		5.07, t (5.1)		

(*c* 0.12, MeOH); UV (MeOH) λ_{max} (log ε) 218 (4.22), 279 (3.51), 289 (3.30) nm; ^{1}H and ^{13}C NMR data, Table 1; ESIMS *m/z* 318.14 $[M+H]^+$, 340.13 $[M+Na]^+$; HRESIMS *m/z* 340.1268 $[M+Na]^+$ (calcd for $C_{16}H_{19}N_3O_4Na$, 340.1268).

(+)-Acrozine C [(+)-**3**]: $[\alpha]_D^{20}$ + 50 (*c* 0.10, MeOH); ECD (0.57 mM, MeOH) λ_{max} ($\Delta\varepsilon$) 209 (–0.86), 233 (+0.66), 270 (–0.37) nm.

(–)-Acrozine C [(–)-**3**]: $[\alpha]_D^{20}$ –42 (*c* 0.07, MeOH); ECD (0.57 mM, MeOH) λ_{max} ($\Delta\varepsilon$) 209 (+1.24), 231 (–0.78), 268 (+0.44) nm.

2.5. X-ray crystallographic analysis

Crystallographic data have been deposited in the Cambridge Crystallographic Data Centre [16]. All crystallographic data were collected on an Agilent Xcalibur Eos Gemini CCD plate diffractometer equipped with graphite-monochromatic Cu Kα radiation (λ = 1.54178 Å) at 293(2) K. The data were corrected for absorption by using the program SADABS [17]. The structure was solved by direct methods and subsequent difference Fourier synthesis and refined by full-matrix least-squares techniques with the SHELXTL software package [18]. All non-hydrogen atoms were refined anisotropically. The H atoms belonging to C atoms were calculated theoretically, and those to O atoms were determined by difference Fourier maps [19].

2.5.1. Crystal data of (±)-*1*

$C_{16}H_{19}N_3O_4S$; fw = 349.40, triclinic space group *P*-1, unit cell dimensions a = 7.4100(8) Å, b = 9.1785(11) Å, c = 12.9144(10) Å, V = 827.89(15) Å^3, α = 72.7000(10)°, β = 80.960(2)°, γ = 85.860(2)°, Z = 2, d_{calcd} = 1.102 mg/m^3, crystal dimensions 0.21 × 0.17 × 0.10 mm^3, μ = 1.970 mm^{-1}, F(0 0 0) = 368. The 4900 measurements yielded 2882 independent reflections after equivalent data were averaged, and Lorentz and polarization corrections were applied. The final refinement gave R_1 = 0.0596 and wR_2 = 0.1416 [$I > 2\sigma(I)$].

2.5.2. Crystal data of (±)-*2*

$C_{16}H_{19}N_3O_4S$; fw = 349.40, triclinic space group *P*-1, unit cell dimensions a = 8.8726(14) Å, b = 10.1438(16) Å, c = 10.8897(17) Å, V = 850.5(2) Å^3, α = 117.470(16)°, β = 96.077(13)°, γ = 96.349(13)°, Z = 2, d_{calcd} = 1.364 mg/m^3, crystal dimensions 0.23 × 0.08 × 0.04 mm^3, μ = 1.918 mm^{-1}, F(0 0 0) = 368. The 4965 measurements yielded 2948 independent reflections after equivalent data were averaged, and Lorentz and polarization corrections were applied. The final refinement gave R_1 = 0.0685 and wR_2 = 0.1370 [$I > 2\sigma(I)$].

2.5.3. Crystal data of (±)-*3*

$C_{16}H_{19}N_3O_4$; fw = 317.34, monoclinic space group *P*2(1)/*n*, unit cell dimensions a = 12.3238(11) Å, b = 7.5865(5) Å, c = 17.4394(16) Å, V = 1614.9(2) Å^3, α = γ = 90°, β = 97.936(2), Z = 4, d_{calcd} = 1.305 mg/m^3, crystal dimensions 0.27 × 0.13 × 0.08 mm^3, μ = 0.789 mm^{-1}, F(0 0 0) = 672. The 5438 measurements yielded 2807 independent reflections after equivalent data were averaged, and Lorentz and polarization corrections were applied. The final refinement gave R_1 = 0.0534 and wR_2 = 0.1187 [$I > 2\sigma(I)$].

2.6. ECD calculations

Conformational searches were performed via molecular mechanics using the MM+ method in HyperChem 8.0 software, and the geometries were further optimized at the B3LYP/6-31G level via Gaussian 09 software to give the energy-minimized conformers. Then, the optimized conformers were subjected to the calculations of ECD spectra using the TDDFT at B3LYP/6-31G level; solvent effects of the MeOH solution were evaluated at the same DFT level using the SCRF/PCM method [20].

2.7. Antimicrobial assay

Antimicrobial evaluation against human pathogenic bacterium (*Escherichia coli*), aquatic pathogens (*Aeromonas hydrophila*, *Micrococcus luteus*, *Pseudomonas aeruginosa*, *Edwardsiella tarda*, *E. ictaluri*, *Vibrio alginolyticus*, *V. harveyi*, *V. parahemolyticus*, *V. anguillarum*, and *V. vulnificus*), and plant-pathogenic fungi (*Alternaria solani*, *Bipolaris sorokiniana*, *Ceratobasidium cornigerum*, *Colletotrichum gloeosporioides*, *C. glecosporioides* Penz, *Coniothyrium diplodiella*, *Fusarium graminerum*, *F. oxysporum*, *F. oxysporum*.sp.*cucumebrium* Owen, *F. oxysporum* f. sp. *momordicae* nov. f., *F. solani*, *Helminthosporium maydis*, *Penicillium digitatum*, *Physalospora piricola*, and *Valsa mali*), were carried out by the microplate assay [21]. The pathogenic bacterium and aquatic pathogenic strains were provided by the Institute of Oceanology, Chinese Academy of Sciences, while the plant pathogenic fungal strains were obtained from Qingdao Agricultural University. Chloramphenicol and

amphotericin B were used as positive controls against bacteria and fungi, respectively.

2.8. Anti-acetylcholinesterase (AChE) assay

Anti-AChE activity was measured by the spectrophotometric method of Ellman modified slightly [22]. Firstly, the compound samples and the positive control tacrine were dissolved in MeOH and diluted to a final concentration range, and the 5 μL sample was added per well in a 96-well microplate. After the solvent being evaporated, the following solvent and reagent were added per well: 50 μL PBS (0.1 M NaH_2PO_4/Na_2HPO_4 buffer, pH 7.4); 10 μL AChE (acetylcholinesterase, from electric eel, 2 U/mL); and 20 μL DTNB (5,5′-dithiobis-(2-nitrobenzoic acid), 5 mM). After in 10 min of incubation at 37 °C, then 20 μL ATCh (acetylthiocholine iodide, 10 mM) was added and, after additional 10 min, the absorbance was read at 405 nm (A_{sample}). Each sample was provided with a sample background and absorbance was determined ($A_{sample\ background}$) using the same method in which ATCh was replaced with PBS. A_{blank} was measured without sample in the same way and blank background containing all of the components except sample (replaced with PBS) and AChE (replaced with BSA, bovine serum albumin, 1 mg/mL) was included in the analyses ($A_{blank\ background}$). Each experiment was assayed in triplicate. AChE inhibition was calculated using Equation:

$$I\% = \frac{(A_{blank} - A_{blank\ background}) - (A_{sample} - A_{sample\ background})}{(A_{blank} - A_{blank\ background})} \times 100\%$$

where I% is the inhibition percentage.

3. Results and discussion

3.1. Structural elucidation of the isolated compounds

The fermentation culture of *A. luteoalbus* TK-43 was exhaustively extracted with ETOAc to afford an extract, which was further purified by a combination of column chromatography on Si gel, Lobar LiChroprep RP-18, and Sephadex LH-20, as well as by semi-preparative HPLC, to yield compounds **1**–**3**.

Compound **1** was initially obtained as a white, amorphous powder. Its molecular formula was determined to be $C_{16}H_{19}N_3O_4S$ on the basis of positive HRESIMS data. The ^{1}H NMR spectroscopic data (Table 1) displayed signals for six methines (one aliphatic, one olefinic, and four aromatic), two aliphatic methylenes, and one thiomethyl and one methoxy groups, as well as three exchangeable protons. The ^{13}C NMR and DEPT data (Table 1) confirmed the presence of 16 carbon atoms with six methines (with five aromatic/olefinic), two methylenes, two methyls (one -SMe and one -OMe), and six nonprotonated (two carbonyl, one aliphatic, and three aromatic/olefinic) carbons. Detailed analysis of the ^{1}H and ^{13}C NMR spectroscopic data revealed that **1** was an IDT derivative similar to c(TrpSer) [23] and chetoseminudin C [24]. However, compound **1** had one more -SMe group than that of c(TrpSer), and one less –SMe group than that of chetoseminudin C, and had one more -OMe group more than any of them. The -SMe group in **1** was assigned at C-6 as supported by HMBC correlation from the protons of -SMe to C-6 (Fig. 2), while the position of -OMe group, either at *N*-2 or at *N*-5, could not be unequivocally assigned due to lack of diagnostic HMBC correlations, and this issue was solved by X-ray crystallographic experiments as discussed later. The relative configuration of **1** was determined by analysis of NOESY data. The key NOE correlations from H-3 to -SMe-6 suggested the cofacial orientation of the two groups (Fig. 3).

To ultimately solve the structure and absolute configuration of compound **1**, efforts toward single crystal analysis were performed. With many attempts, quality crystals were obtained by dissolving the samples in the solvents CH_2Cl_2–MeOH (1:1) followed by slow evaporation under refrigerator in two weeks. The planar structure of compound **1** including the connection of -OMe to *N*-2 was thus unambiguously established by a single-crystal X-ray diffraction experiment using Cu Kα radiation (Fig. 4). Surprisingly, the X-ray crystal data (Supplementary material) indicated that the crystal of **1** had a *P*-1 space group with no Flack parameter, suggesting that compound **1** was a racemic mixture with two enantiomers that having identically NMR data. The racemic nature of compound **1** was also confirmed by its specific optical rotation ($[\alpha]_D^{20}$ 0 (*c* 0.08, MeOH)), and by the fact that no Cotton Effects (CEs) could be observed in the ECD spectrum as well (Fig. S8). The optical resolution of **1** by chiral HPLC afforded two enantiomers, (+)-**1** and (–)-**1** (Fig. S9), which showed mirror curves in their ECD spectra (Fig. S10 and S11). The absolute configuration of (+)-**1** was established by ECD quantum chemical calculations in Gaussian 09 [20]. The experimental ECD spectrum for (+)-**1** showed excellent agreement with the calculated (3*R*, 6*S*)-absolute configuration of (+)-**1** (Fig. 5) which was computed with the time-dependent density function theory (TD-DFT) method at the gas-phase B3LYP/6-31G(d) level. On the other hand, compound (–)-**1**, which showed almost completely opposite experimental ECD spectrum as that of (+)-**1**, was assigned the absolute configuration as 3*S* and 6*R*. On the basis of the above evidence, the structures of (+)-**1** and (–)-**1** which were respectively named as (+)-acrozine A and (–)-acrozine A were determined.

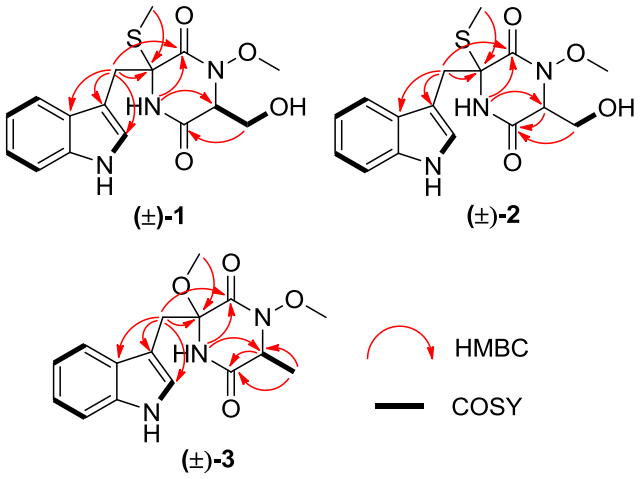

Fig. 2. COSY and key HMBC correlations of compounds (±)-**1** ~ (±)-**3**.

Compound **2**, obtained as a white, amorphous powder, was determined to possess the molecular formula $C_{16}H_{19}N_3O_4S$, same as that of compound **1**, on the basis of HRESIMS data. Its NMR spectroscopic data were nearly identical to those of **1** except for the ^{1}H NMR signals of H-3 (δ_H 3.50 in **2** *vs* δ_H 4.37 in **1**) and the -OMe group (δ_H 3.19 in **2** *vs* δ_H 3.67 in **1**), which might be affected by the position of the -OMe group or the configuration of chiral carbons (C-3 and/or C-6). Although the -OMe group could again not be unambiguously assigned at *N*-2 or *N*-5 due to lack of HMBC correlations, a single crystal of **2** was successfully cultivated upon slow evaporation of the solvent (CH_2Cl_2–MeOH, 1:1) by storing the sample in a refrigerator for two weeks, and making an feasible X-ray diffraction analysis of compound **2** (Fig. 4) that unequivocally confirmed the position of the -OMe at *N*-2. The relative configuration of **2** was also deduced from NOE correlations between the protons of -SMe-2 and OH-15, which placed these groups on the same face of the molecule (Fig. 3), and the single-crystal X-ray diffraction experiment further proved this deduction (Fig. 4).

The crystal of compound **2** also had a *P*-1 space group, which indicated its racemic nature. This was also demonstrated by the specific optical rotation of **2**, $[\alpha]_D^{20}$ 0 (*c* 0.10, MeOH) and the absence of maximum peaks in the ECD spectrum as well (Fig. S20). Chiral HPLC separation of compound **2** afforded a pair of enantiomers, (+)-**2** and (–)-**2** (Fig. S21). The TDDFT ECD spectrum calculated for 3*S* and 6*S* absolute

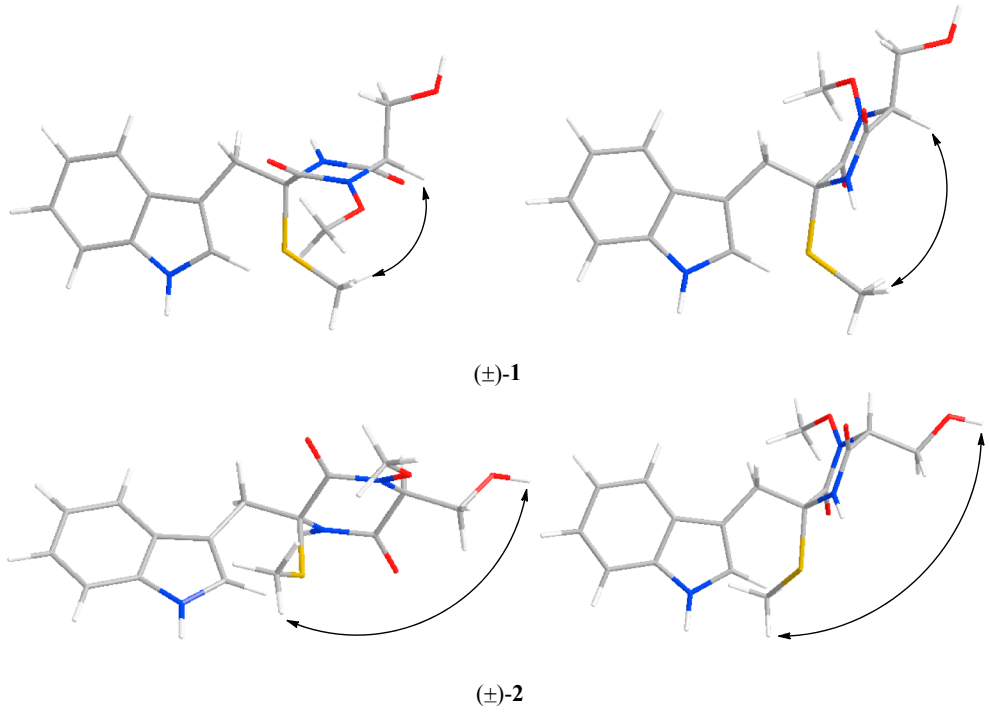

Fig. 3. Key NOESY correlations of compounds (±)-**1** and (±)-**2**.

configuration in (+)-**2** gave good agreement with the experimental curve (Fig. 5). Meanwhile, the absolute configuration of (–)-**2**, as an enantiomer of (+)-**2,** was determined as 3*R* and 6*R*. Compound (+)-**2** and (–)-**2** were assigned the trivial names (+)-acrozine B and (–)-acrozine B, respectively.

Compound **3** was originally obtained as a white, amorphous powder and had the molecular formula $C_{16}H_{19}N_3O_4$ as determined by HRESIMS data, having one *S*-atom less than **1**. Detailed analysis of the NMR data suggested that compound **3** had the same basic structure as that of **1** and *cyclo*-(L-Trp-L-Ala) [25]. However, the –SMe and $–CH_2OH$ groups in **1** were replaced by –OMe and –Me groups in **3**, respectively, and, when comparing to that of *cyclo*-(L-Trp-L-Ala), compound **3** had two -OMe substitutions, with one attached at C-6 and another one connected at *N*-2 or *N*-5. The NMR data of **3** (Table 1) as well as the COSY and HMBC correlations (Fig. 2) supported this deduction. However, the position of one of the two –OMe groups, either at *N*-2 or at *N*-5, could again not be assigned due to lack of diagnostic HBMC correlation, whereas the relative configuration at C-3 and C-6 could also not be resolved by NOESY experiment since overlapping of the ^{1}H NMR signals of two –OMe groups.

Efforts to get crystals of compound **3** was also successfully performed, and its structure and relative configuration were thus resolved by a single-crystal X-ray diffraction experiment using Cu Kα radiation (Fig. 4).

By the X-ray diffraction analysis (the crystal of **3** had a $p2_1/n$ space group), the optical rotation determination ($[\alpha]_D^{20}$ 0 (*c* 0.12, MeOH), and the ECD measurement (Fig. S32), compound **3** was also revealed as a racemate. Separation of **3** yielded (+)-**3** and (–)-**3** by the chiral HPLC in a ratio of 1:1 (Fig. S33), which were individually determined absolute configurations by ECD quantum chemical calculations (Fig. 5), and assigned (+)-**3** as (3*S*, 6*S*) and (–)-**3** as (3*R*, 6*R*). The trivial names, (+)-acrozine C and (–)-acrozine C, were assigned to them, respectively.

Compounds **1–3** contain *N*-methoxy group in their molecules which is infrequent in previously reported IDTs. A question thus arises immediately as to whether they occurred naturally or were obtained as artifacts of the purification procedures. To solve this problem, HPLC profiles of the crude extract and the isolated compounds were rechecked and compared. Compounds **1** and **2**, which were obtained in larger amount than that of **3**, could be obviously detected in the initial crude extract of the fungal culture (Fig. S38), suggesting that compounds **1** and **2** were not formed during the purification steps, whereas compound **3**, the minor constituent, could not be clearly detected in the HPLC profile of the crude extract, possibly due to the overlapping of the peak with other components. Although the artifact nature could not be completely ruled out, the above evidence supports a natural source for compounds **1–3**.

3.2. Anti-microbial and anti-acetylcholinesterase activity of the isolated compounds

Compounds **1–3** were evaluated for antimicrobial activity against human pathogenic bacterium, aquatic pathogens, and plant-pathogenic fungi. None of them exhibited activity against the pathogenic bacteria at a concentration of 64 μg/mL. Compound (–)-**2** showed activity against the plant pathogen *Fusarium solani* with MIC values of 32 μg/mL, which is more potent than that of its enantiomer (+)-**2** and its epimers (+)-**1** and (–)-**1** (MIC > 64 μg/mL).

Compounds **1–3** were further evaluated for *in vitro* anti-acetylcholinesterase (AChE) activity. The results showed that (±)-**1** had modest activity with IC_{50} value 9.5 μM (Table 2), and after chiral resolution, (+)-**1** (IC_{50} = 2.3 μM) showed better activity than that of (–)-**1** (IC_{50} = 13.8 μM) and (±)-**1**. None of the tested compounds had stronger activities than that of the positive control tacrine (IC_{50} = 0.14 μM). It can be seen from these biological activity data that compounds with same planar structure may exhibit different biological activity and the selectivity of activity is related to the absolute configuration. Compound (+)-**1** (with 3*R*, 6*S*) and (–)-**1** (with 3*S*, 6*R*) exhibited better activities than that of (+)-**2** (with 3*S*, 6*S*) and (–)-**2**

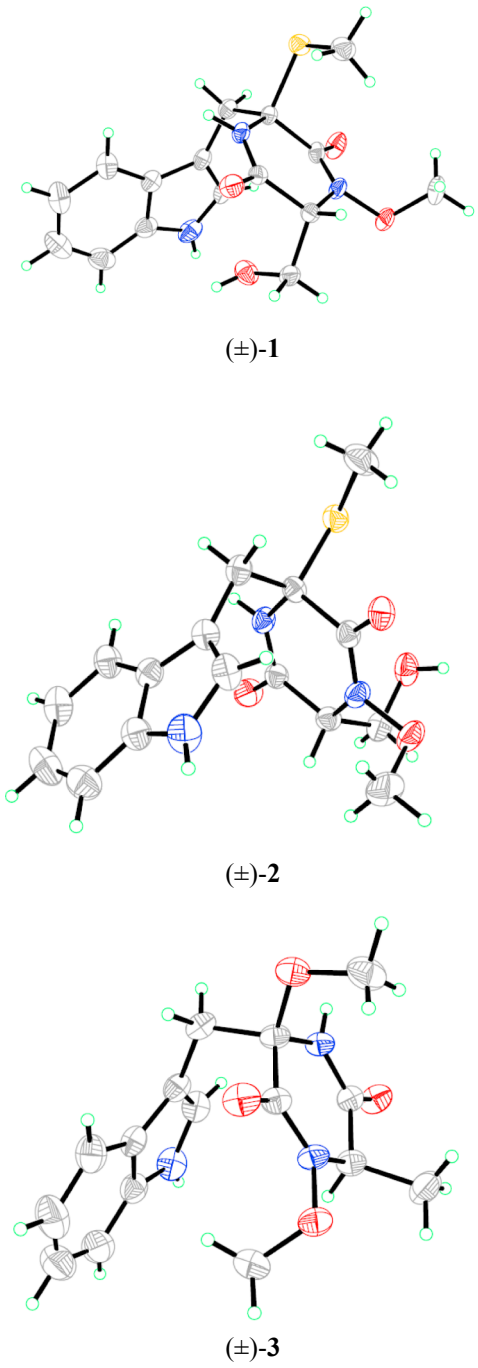

Fig. 4. X-ray crystallographic structures of compounds (±)-**1** ~ (±)-**3**.

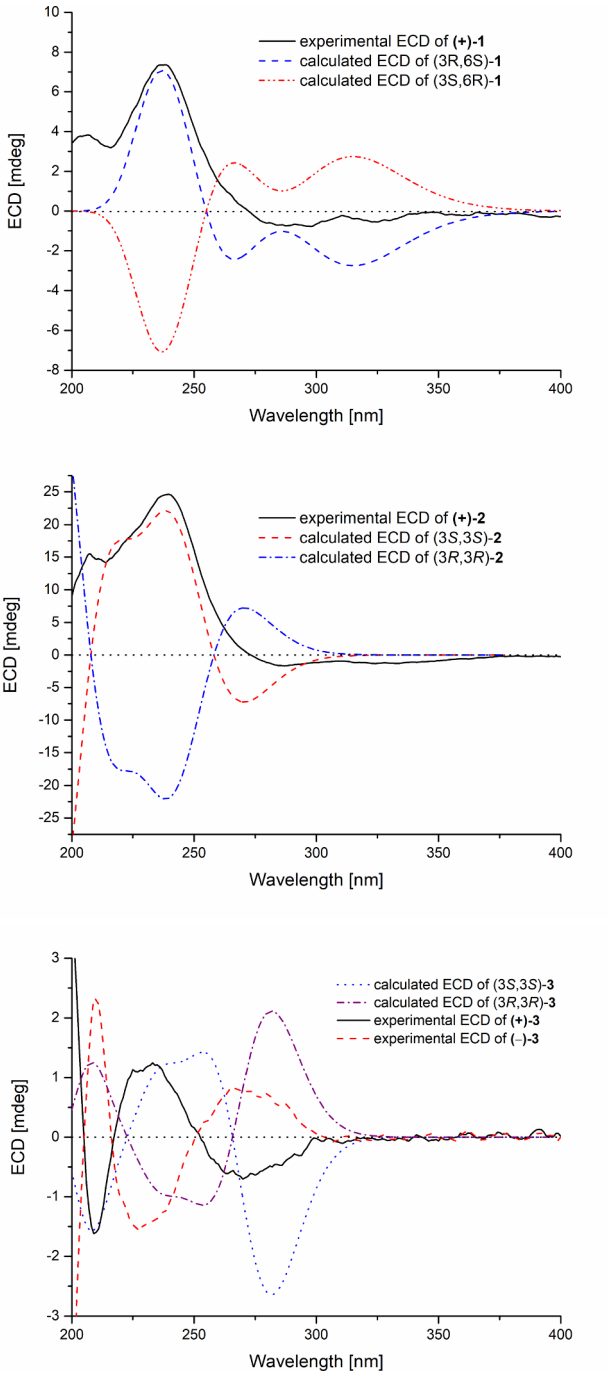

Fig. 5. Experimental and calculated ECD spectra of compounds (+)-**1** ~ (+)-**3** and (–)-**3**.

(with 3*R*, 6*R*), suggesting that compounds with different absolute configurations at C-3 and C-6 have stronger anti-AChE activity than those with same absolute configurations at C-3 and C-6. In addition, it is likely that the absolute configuration of C-3 significantly affect the anti-AChE activity, as evidenced that compounds (+)-**1**, (–)-**2**, and (–)-**3** (with 3*R*) showed better activity than that of (–)-**1**, (+)-**2**, and (+)-**3** (with 3*S*), respectively.

4. Conclusion

In summary, three pairs of infrequent *N*-methoxy-containing indolediketopiperazine enantiomers, (±)-acrozines A–C (**1–3**), were isolated from the culture extract of *Acrostalagmus luteoalbus* TK-43 obtained from the marine green alga *Codium fragile*. This is the first report of indolediketopiperazines containing *N*-OMe group from the fungal species of the genus *Acrostalagmus*. The resolution of the enantiomers (±)-(**1**) – (±)-(**3**) was successfully performed by chiral HPLC and compound (+)-**1** exhibited modest activity against acetylcholinesterase with IC_{50} value 2.3 μM, which was better than that of (–)-**1** and (±)-**1**.

Declaration of Competing Interest

The authors declare no competing financial interest.

Table 2
IC_{50} of compounds (±)-**1** ~ (±)-**3** of acetylcholinesterase (AChE) inhibition assay.

Compound	(±)-**1**	(+)-**1**	(–)-**1**	(±)-**2**	(+)-**2**	(–)-**2**	(±)-**3**	(+)-**3**	(–)-**3**	Tacrine
IC_{50} (μM)	9.5	2.3	13.8	60.7	78.8	49.2	130.5	160.6	121.7	0.14

Acknowledgements

This work was financial supported by the National Natural Science Foundation of China (NSFC grant 81673351 and 31330009) and by the European Commission under the program "Marie Curie Actions-International Research Staff Exchange Scheme" (IRSES, Grant Agreement Number: PIRSES-GA-2011-295226). B.-G.W. appreciates the support of Taishan Scholar Project from Shandong Province of China.

Appendix A. Supplementary material

Supplementary data to this article can be found online at https://doi.org/10.1016/j.bioorg.2019.103030.

References

[1] J.W. Blunt, A.R. Carroll, B.R. Copp, R.A. Davis, R.A. Keyzers, M.R. Prinsep, Nat. Prod. Rep. 35 (2018) 8–35.
[2] N.Y. Ji, B.G. Wang, Fungal Divers. 80 (2016) 301–342.
[3] Y.P. Song, Z.Z. Shi, F.P. Miao, S.T. Fang, X.L. Yin, N.Y. Ji, Org. Lett. 20 (2018) 6306–6309.
[4] J.J. Wang, F.M. Chen, Y.H. Liu, Y.X. Liu, K.L. Li, X.L. Yang, S.W. Liu, X.F. Zhou, J. Yang, J. Nat. Prod. 81 (2018) 2722–2730.
[5] Y.P. Song, S.T. Fang, F.P. Miao, X.L. Yin, N.Y. Ji, J. Nat. Prod. 81 (2018) 2553–2559.
[6] Z.Z. Shi, F.P. Miao, S.T. Fang, X.L. Yin, N.Y. Ji, J. Nat. Prod. 81 (2018) 1121–1124.
[7] Y.P. Song, X.H. Liu, Z.Z. Shi, F.P. Miao, S.T. Fang, N.Y. Ji, Phytochemistry 152 (2018) 45–52.
[8] Z.Z. Shi, S.T. Fang, F.P. Miao, X.L. Yin, N.Y. Ji, Bioorg. Chem. 81 (2018) 319–325.
[9] S.Q. Yang, X.M. Li, X. Li, L.P. Chi, B.G. Wang, Mar. Drugs 16 (2018) 114.
[10] H.L. Li, X.M. Li, X. Li, C.Y. Wang, H. Liu, M.U. Kassack, L.H. Meng, B.G. Wang, J. Nat. Prod. 80 (2017) 162–168.
[11] P. Zhang, A. Mándi, X.M. Li, F.Y. Du, J.N. Wang, X. Li, T. Kurtán, B.G. Wang, Org. Lett. 16 (2014) 4834–4837.
[12] F.Z. Wang, Z. Huang, X.F. Shi, Y.C. Chen, W.M. Zhang, X.P. Tian, J. Li, S. Zhang, Bioorg. Med. Chem. Lett. 22 (2012) 7265–7267.
[13] G.H. Yu, Y.J. Wang, R.L. Yu, Y.Y. Feng, L. Wang, Q. Che, Q.Q. Gu, D.H. Li, J. Li, T.J. Zhu, RSC Adv. 8 (2018) 53–58.
[14] L. Li, D. Li, Y. Luan, Q.Q. Gu, T.J. Zhu, J. Nat. Prod. 75 (2012) 920–927.
[15] S. Wang, X.M. Li, F. Teuscher, D.L. Li, A. Diesel, R. Ebel, P. Proksch, B.G. Wang, J. Nat. Prod. 69 (2006) 1622–1625.
[16] Crystallographic data of compounds (±)-1 ~ (±)-3 have been deposited in the Cambridge Crystallographic Data Centre as CCDC 1870549, 1870553, and 1870551, respectively. These data can be obtained free of charge via < http://www.ccdc.cam.ac.uk/ > data request/cif (or from the CCDC, 12 Union Road, Cambridge CB21EZ, U.K.; fax: +44-1223-336-033; e-mail: deposit@ccdc.cam.ac.uk).
[17] G.M. Sheldrick, SADABS, Software for Empirical Absorption Correction, University of Gottingen, Germany, 1996.
[18] G.M. Sheldrick, SHELXTL, Structure Determination Software Programs, Bruker Analytical X-ray System Inc., Madison, WI, 1997.
[19] G.M. Sheldrick, SHELXL-97 and SHELXS-97, Program for X-ray crystal structure solution and refinement, University of Gottingen, Germany, 1997.
[20] M.J. Frisch, G.W. Trucks, H.B. Schlegel, G.E. Scuseria, M.A. Robb, J.R. Cheeseman, G. Scalmani, V. Barone, B. Mennucci, G.A. Petersson, H. Nakatsuji, M. Caricato, X. Li, H.P. Hratchian, A.F. Izmaylov, J. Bloino, G. Zheng, J.L. Sonnenberg, M. Hada, M. Ehara, K. Toyota, R. Fukuda, J. Hasegawa, M. Ishida, T. Nakajima, Y. Honda, O. Kitao, H. Nakai, T. Vreven, J.A. Montgomery Jr., J.E. Peralta, F. Ogliaro, M. Bearpark, J.J. Heyd, E. Brothers, K.N. Kudin, V.N. Staroverov, T. Keith, R. Kobayashi, J. Normand, K. Raghavachari, A. Rendell, J.C, Burant, S.S. Iyengar, J. Tomasi, J.; Cossi, N. Rega, J.M. Millam, M. Klene, J.E. Knox, J.B. Cross, V. Bakken, C. Adamo, J. Jaramillo, R. Gomperts, R.E. Stratmann, O. Yazyev, A.J. Austin, R. Cammi, C. Pomelli, J.W. Ochterski, R.L.; Martin, K. Morokuma, V.G. Zakrzewski, G. A. Voth, P. Salvador, J.J. Dannenberg, S. Dapprich, A.D. Daniels, O. Farkas, J.B. Foresman, J.V.; Ortiz, J. Cioslowski, D.J. Fox, Gaussian 09, Revision C.01; Gaussian, Inc.: Wallingford, CT, 2010.
[21] C.G. Pierce, P. Uppuluri, A.R. Tristan, F.L. Wormley Jr., E. Mowat, G. Ramage, J.L. Lopez-Ribot, Nat. Protoc. 3 (2008) 1494–1500.
[22] G.L. Ellman, K.D. Courtney, V. Andres Jr, R.M. Featherstone, Biochem. Pharmacol. 7 (1961) 88–95.
[23] M. Tullberg, K. Luthman, M. Grøtli, J. Comb. Chem. 8 (2016) 915–922.
[24] H. Fujimoto, M. Sumino, E. Okuyama, M. Ishibashi, J. Nat. Prod. 67 (2004) 98–102.
[25] E. Caballero, C. Avendano, J.C. Menendez, Tetrahedron: Asymmetry 9 (1998) 967–981.